SUPPLEMENTAL FIGURES AND FIGURE LEGENDS:

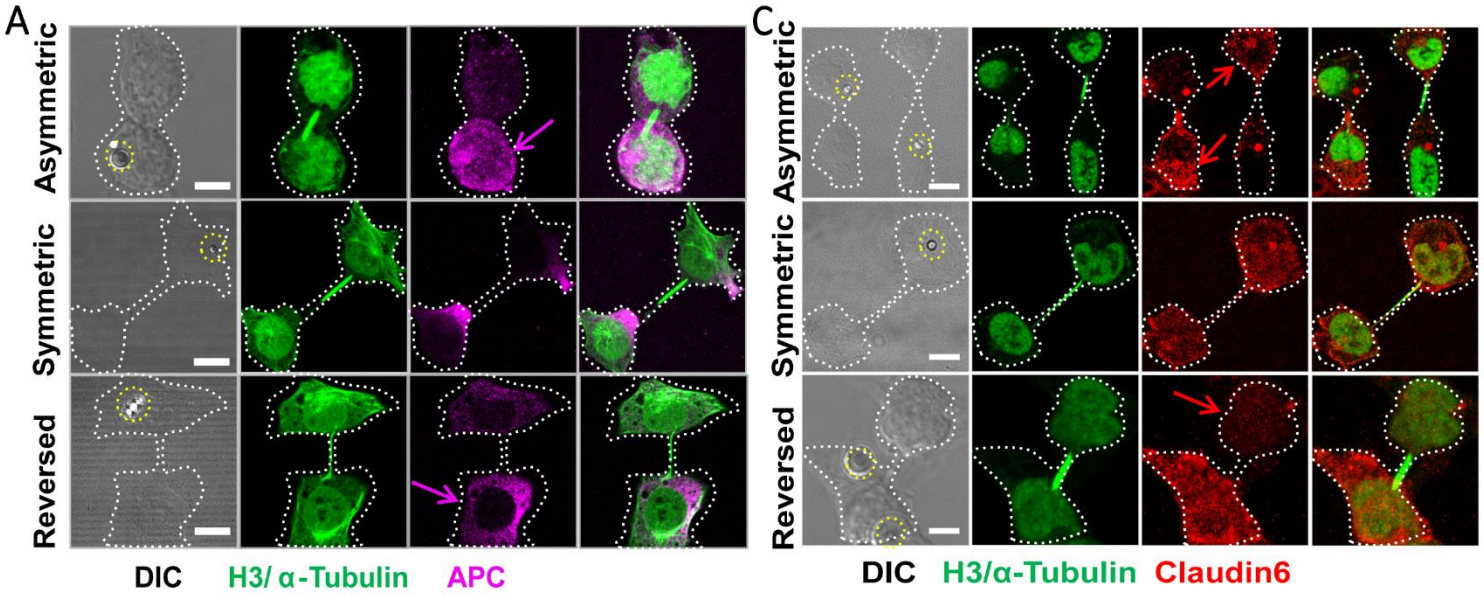

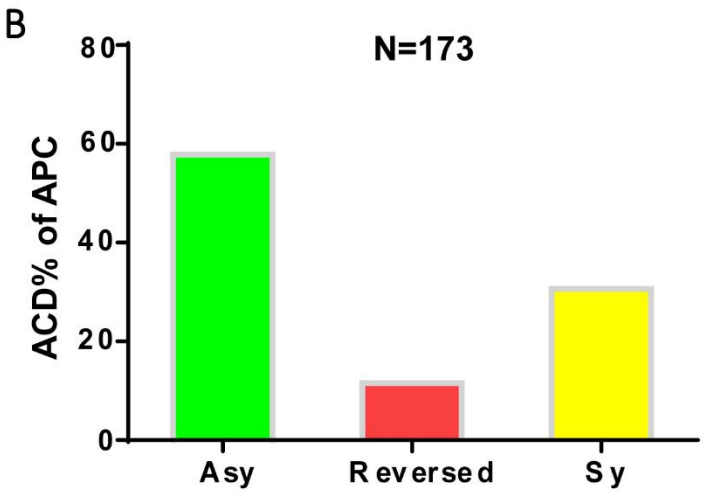

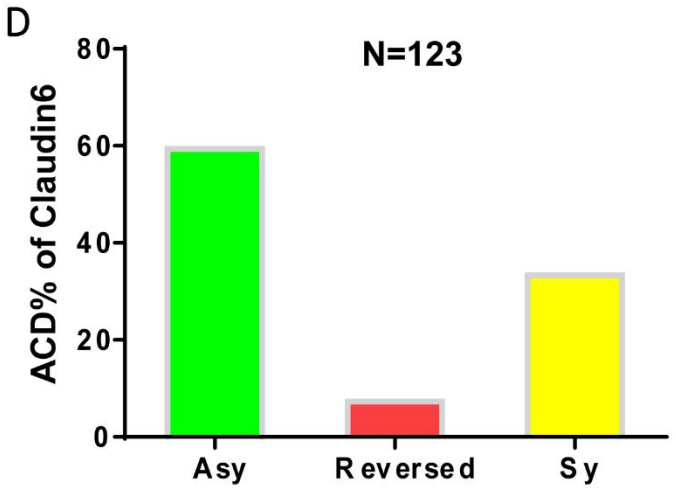

Figure S1: Wnt3a beads induce ACD of *H3-Dendra2* transgenic mESCs. **Related to Figure 1.** (**A**) Representative images of mitotic (telophase) or post-mitotic mESCs carrying *H3-Dendra2* transgene with Wnt3a beads and immunostained with antibodies against α-Tubulin (green) and APC (Magenta). H3-Dendra2 fusion protein (green). Yellow dotted circles outline the position of Wnt3a beads. Magenta arrows indicate the proximal side toward Wnt3a bead. All three patterns are shown: asymmetric, symmetric and reversed asymmetric. (**B**) The corresponding ratios of asymmetric (57.80%), symmetric (30.64%) and reversed asymmetric (11.56%) cell division patterns (*N*= 173). (**C**) Representative images of mitotic (telophase) or post-mitotic mESCs carrying *H3-Dendra2* transgene with Wnt3a beads and immunostained with antibodies against α-Tubulin (green) and Claudin6 (Red). H3-Dendra2 fusion protein (green). Yellow dotted circles outline the position of Wnt3a beads. Red arrows indicate the distal side from Wnt3a bead. All three patterns are shown: asymmetric, symmetric and reversed asymmetric. (**D**) The corresponding ratios of asymmetric (59.35%), symmetric (33.33%) and reversed asymmetric (7.32%) cell division patterns (*N*= 123). Scale bars in (**A**) and (**C**): 5 μm.

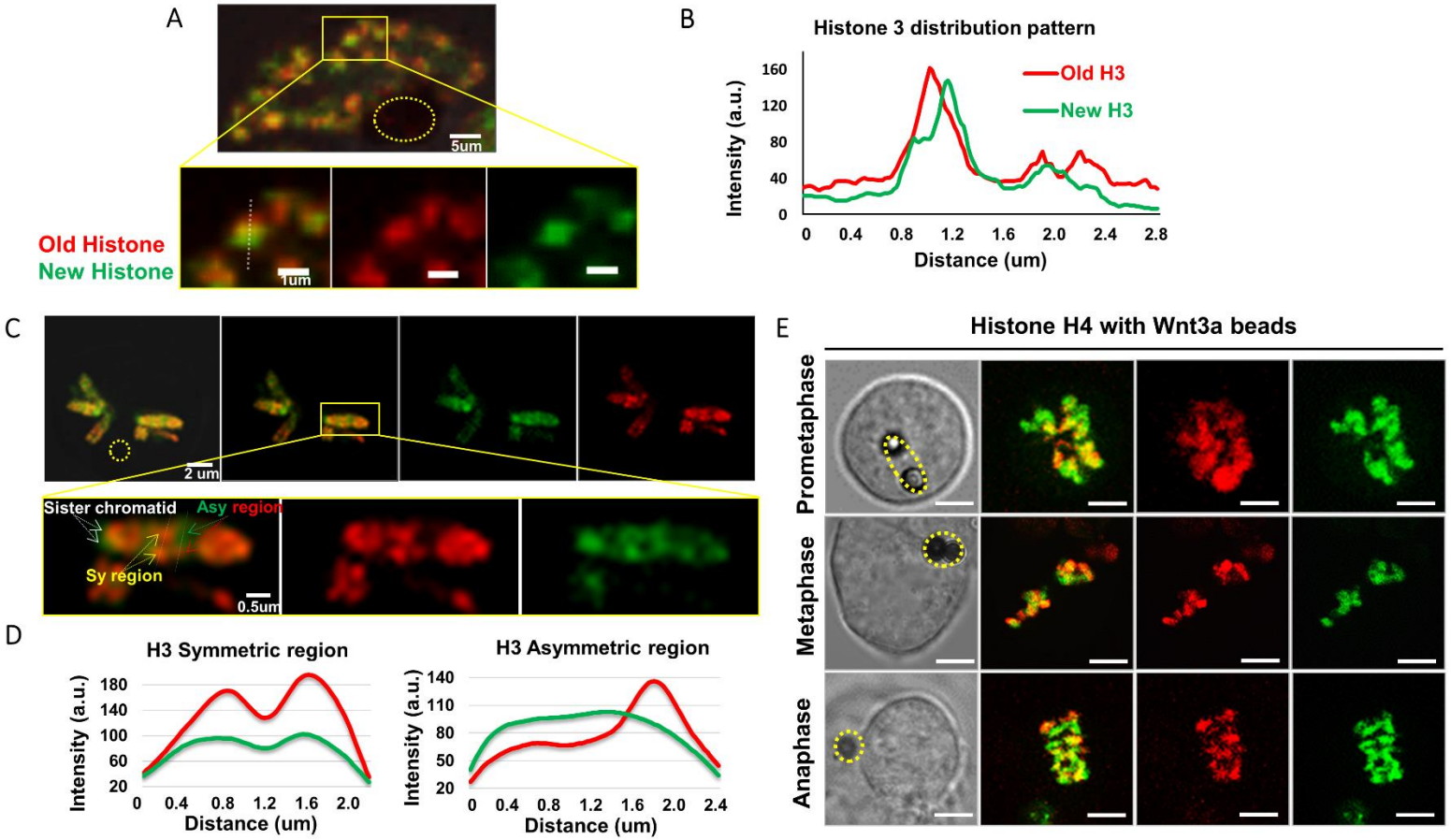

Figure S2: Local non-overlapping old *versus* new histone H3 and H4 distribution in mitotic mESCs with Wnt3a beads. Related to Figure 1. (**A**) Non-overlapping subdomains of old (red) *versus* new (green) histone H3 in a prophase mESC during the second mitosis after photoconversion (Figure 1C), in the presence of Wnt3a beads. (**B**) The line plots at these regions shows non-overlapping

peaks of old H3 *versus* new H3 were separable at approximately 0.25μm (250 nm), which is above the spatial resolution of confocal light microscopy at 200-230nm. (**C**) Non-overlapping subdomains of old H3 *versus* new H3 in a prometaphase mESC during the second mitosis after photoconversion of histone-Dendra2 (Figure 1C), in the presence of Wnt3a beads. (**D**) The line plots show both symmetric and asymmetric old H3 *versus* new H3 domains between condensed sister chromatids. (**E**) Non-overlapping subdomains of old (red) *versus* new (green) histone H4 in mESCs at prometaphase, metaphase, and anaphase mESCs, during the second mitosis after photoconversion of histone-Dendra2 (Figure 1C), in the presence of Wnt3a beads. Yellow dotted circles outline the position of Wnt3a beads in (**A**), (**C**) and (**E**). Scale bars in (**A**) and (**E**): 5 μm; (**C**): 2 μm. Scale bars in (**A**) inset: 1 μm; (**C**) inset: 0.5 μm.

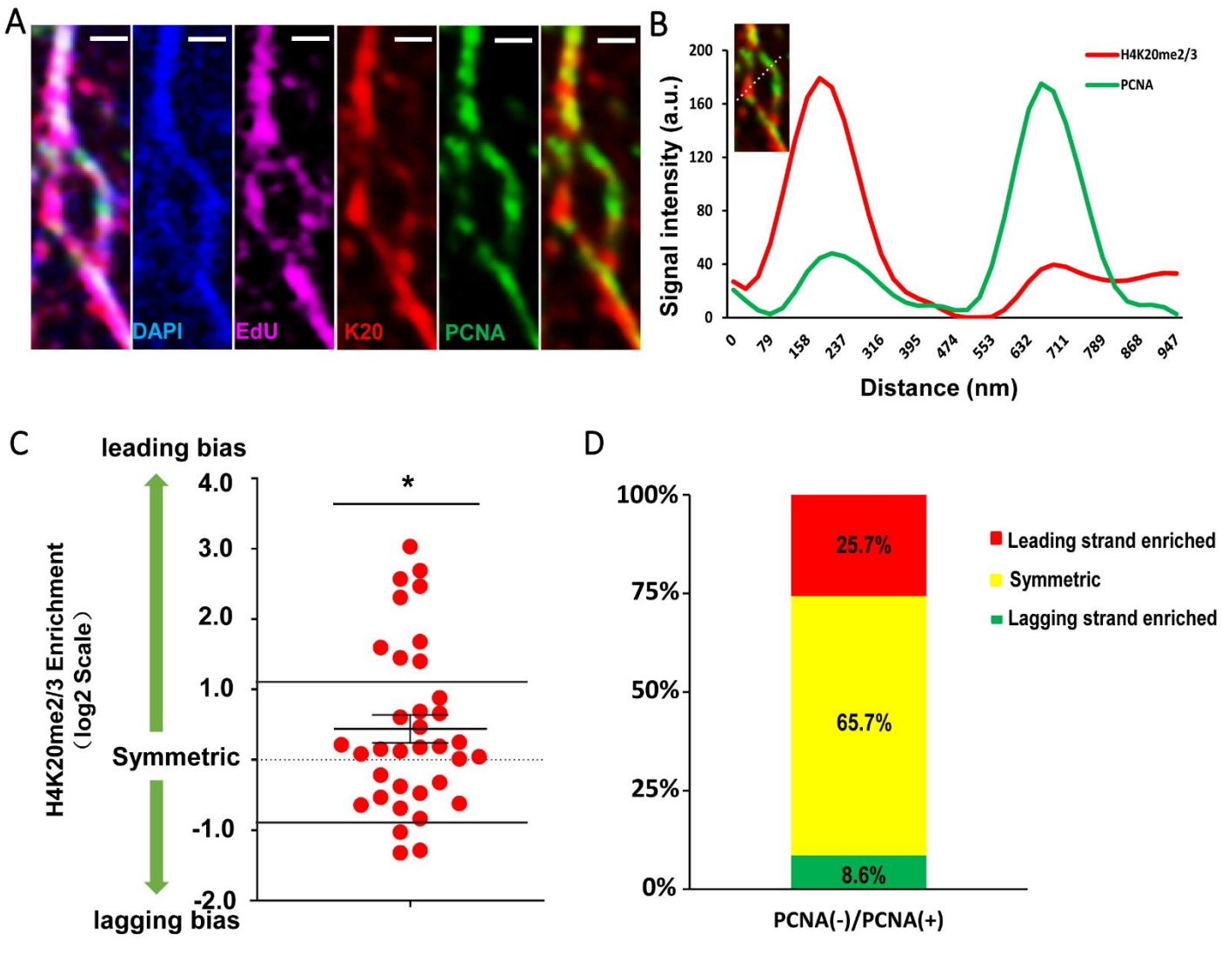
A
DAPI
EdU
K20
PCNA
B
H4K20me2/3
PCNA
Signal intensity (a.u.)
200
160
120
80
40
0
0
79
158
237
316
395
474
553
632
711
789
868
947
Distance (nm)
C
leading bias
4.0
3.0
2.0
1.0
Symmetric
-1.0
-2.0
lagging bias
H4K20me2/3 Enrichment
（log2 Scale）
*
D
100%
75%
50%
25%
0%
25.7%
65.7%
8.6%
Leading strand enriched
Symmetric
Lagging strand enriched
PCNA(-)/PCNA(+)

Figure S3: Old histone-enriched H4K20me2/3 shows preferentially leading-strand distribution on chromatin fibers from mESCs with Wnt3a beads. Related to Figure 2. (**A**) Airyscan images of chromatin fiber labeled with EdU (magenta) to show the replicative regions with asymmetric distribution of H4K20me2/3 (red) and PCNA (green) at the opposite strands. DNA label DAPI (blue). (**B**) The line plots show the leading strand-enriched (i.e. PCNA-less side) H4K20me2/3 distribution between replicative sister chromatids that is separable in (**A**). (**C**) Quantification of the $\log_2$ (H4K20me2/3 signal at PCNA-less leading strand/ H4K20me2/3 signal at PCNA-enriched lagging strand) using chromatin fibers from mESCs without Wnt3a beads. The average $\log_2$ ratio= 0.4393± 0.1984 (average ± SEM, *N*= 35 replicative chromatin fibers), which is significantly different from the symmetric distribution pattern with $\log_2$ ratio= 0. * *P*<0.05 based on Mann-Whitney test. Two dotted lines indicate the symmetric range for H4K20me2/3 distribution between sister chromatids [see STAR methods and (Wooten et al., 2019) to define this range]. (**D**) The percentages of leading strand enriched ($\log_2$ ratio >1.025, ratio>2.035), symmetric (-0.953< $\log_2$ ratio <1.025, 0.517< ratio<2.035) and lagging strand enriched ($\log_2$ ratio <-0. 953, ratio<0.517) using data points from (**C**). Scale bars in (**A**): 500 nm.

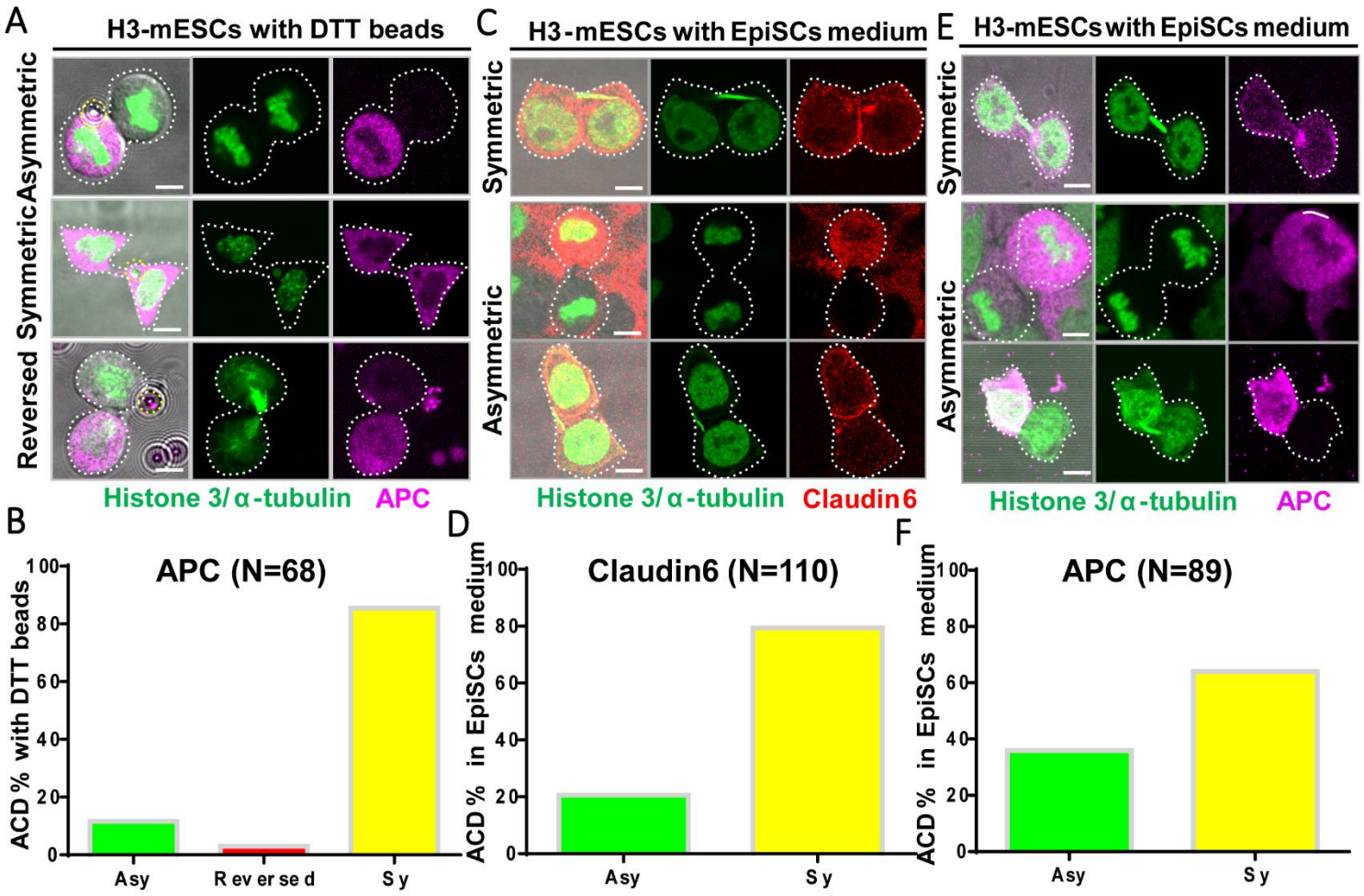

Figure S4: Decreased ACD of mESCs with DTT-inactivated Wnt3a beads or in differentiation-promoting EpiSC medium.

Related to Figure 3 and 4. (**A**) Representative images of mitotic (telophase) or post-mitotic mESCs carrying *H3-Dendra2* transgene

with Wnt3a beads treated with DTT and immunostained with antibodies against APC (Magenta), H3-Dendra2 fusion protein (green). Yellow dotted circles outline the position of Wnt3a beads. All three patterns are shown: asymmetric, symmetric and reversed asymmetric. (**B**) The corresponding ratios of asymmetric (11.63%), symmetric (85.42%) and reversed asymmetric (2.95%) cell division patterns (*N*= 68) for mESCs with DTT-treated Wnt3a beads. Compared to the percentage using active Wnt3a beads (57.80%, Figure S1B), the asymmetric pattern for mESCs with DTT-treated Wnt3a beads is significantly decreased ($P< 10^{-4}$ based on Fisher exact probability test). (**C**) Representative images of mitotic (telophase) or post-mitotic cells carrying *H3-Dendra2* transgene cultured with EpiSC medium that promotes differentiation and immunostained with antibodies against α-Tubulin (green) and Claudin6 (Red). H3-Dendra2 fusion protein (green). Both symmetric and asymmetric patterns are shown. (**D**) The corresponding ratios of asymmetric (20.62%) and symmetric (79.38%) cell division patterns (*N*= 110) for mESCs cultured with EpiSC medium. (**E**) Representative images of mitotic (telophase) or post-mitotic cells carrying *H3-Dendra2* transgene cultured with the EpiSC medium that promotes differentiation and immunostained with antibodies against α-Tubulin (green) and APC (Magenta). H3-Dendra2 fusion protein (green). Both symmetric and asymmetric patterns are shown. Both asymmetric and symmetric patterns are shown. (**F**) The corresponding ratios of asymmetric (35.96%) and symmetric (64.04%) cell division patterns (*N*= 89) for mESCs cultured with EpiSC medium. The reversed asymmetric distribution pattern is not applicable under this condition without the Wnt3a beads in (**C-D**) and (**E-F**). The percentages of asymmetric division pattern for mESCs in EpiSC medium were significantly lower than that for mESCs with Wnt3a beads in CM+LIF+2i (Figure S4F *versus* Figure S1B: $P< 10^{-4}$; and Figure S4D *versus* Figure S1D: $P< 10^{-3}$, based on Fisher exact probability test). Scale bars in (**A**), (**C**) and (**E**): 5 μm.